CHEMISTRY
A EUROPEAN JOURNAL

DOI: 10.1002/chem.200601873

The Heteropolytungstate Core $\{BW_{13}O_{46}\}^{11-}$ Derived as Monomer, Dimer, and Trimer

Nathalie Leclerc-Laronze,[a] Jérôme Marrot,[a] Gilbert Hervé,[a] René Thouvenot,*[b] and Emmanuel Cadot*[a]

Dedicated to Professor Michael Thor Pope on the occasion of his retirement

Abstract: A study of the borotungstate system has led to the characterization of new, original compounds based on the unconventional Keggin derivative $[H_3BW_{13}O_{46}]^{8-}$ ion (denoted as **1**). $[H_3BW_{14}O_{48}]^{6-}$ (**2**) and the dimer $[H_6B_2W_{26}O_{90}]^{12-}$ (**3**) crystallize as mixed cesium/ammonium salts and have been characterized by single-crystal X-ray diffraction analysis. Anion **2** reveals an unusual arrangement, consisting of an outer $\{W_3O_9\}$ core grafted onto the monovacant $[BW_{11}O_{39}]^{9-}$ Keggin moiety and exhibits an unprecedented distorted square-pyramidal arrangement for a *cis*-$\{WO_2\}$ core. Elemental analysis, supported by bond distance analysis, is consistent with the presence of three protons distributed over the terminal oxygens of the outer $\{W_3O_7\}$ capping fragment. The $[H_6B_2W_{26}O_{90}]^{12-}$ ion (**3**) is formally derived from the direct condensation of two $[H_3BW_{13}O_{46}]^{8-}$ subunits. The cisoid arrangement of the two $[BW_{11}O_{39}]^{9-}$ subunits, coupled with the antiparallel arrangement of the two quasi-linear O=W···O=W−OH_2 chains within the central $\{W_4O_{12}\}$ connecting group, breaks any symmetry, thereby resulting in a chiral compound. Polarography and pH-metric titrations reveal the formation of the monomeric precursor $[H_3BW_{13}O_{46}]^{8-}$ (anion **1**) under stoichiometric conditions. ^{183}W NMR analysis of **2** and **3** in solution gives complex spectra, consistent with the presence of equilibria between several species. In the frame of this study, we also report on a structural re-investigation of the $[H_6B_3W_{39}O_{132}]^{15-}$ ion (**4**) based on reliable results obtained in the solid state by means of single-crystal X-ray diffraction analysis, and in solution by means of 1D and 2D COSY ^{183}W NMR. X-ray diffraction analysis revealed the presence of three attached aquo ligands on the central $\{W_6O_{15}\}$ connecting core, generating three O=W···O=W−OH_2 quasi-linear chains, which are responsible for the chirality of the trimeric assembly. This structural arrangement accounts for the 39-line ^{183}W solution spectrum. The 2D COSY spectrum permits reliable assignments of the six strongly shielded resonances (around −250 and −400 ppm) to the six central W atoms, as well as additional assignments. The origin of such strong shielding for these particular W atoms is discussed on the basis of previously published results. Infrared data for compounds **1**, **3**, and **4** are also presented.

Keywords: boron · cluster compounds · NMR spectroscopy · polyoxometalates · tungsten

Introduction

Polyoxometalates have stimulated many current research activities in broad domains of science, such as catalysis, medicine, and materials.[1] This class of molecular materials offers the possibility of stereospecifically combining elements, mainly transition metal cations, in structurally diverse multiunit compounds. This enormous potential has led to the generation of numerous compounds with specific targeted properties, such as magnetic properties, redox activity, or level of acidity, for anticipated applications in many areas. The rich diversity of the lacunary polytungstates makes them attractive for use as rigid ligands.[2,3] This class of anionic ligands,

[a] Dr. N. Leclerc-Laronze, Dr. J. Marrot, Prof. G. Hervé, Prof. E. Cadot
Université de Versailles Saint Quentin, Institut Lavoisier de Versailles, ILV, UMR CNRS 8180
45 Avenue des Etats-Unis, 78035 Versailles Cedex (France)
Fax: (+33) 139-254-382
E-mail: cadot@chimie.uvsq.fr

[b] Dr. R. Thouvenot
Université Pierre et Marie Curie-Paris 6, Institut de Chimie Moléculaire FR 2769, Laboratoire de Chimie Inorganique et Matériaux Moléculaires, UMR CNRS 7071
4, Place Jussieu, Case 42, 75252 Paris Cedex 05 (France)
Fax: (+33) 144-273-841
E-mail: rth@mailhost.ccr.jussieu.fr

ranging from monovacant to hexavacant anions, exhibits various polyhedral arrangements, which are mainly derived from the most common archetypal structural motifs, that is, Dawson or Keggin structures.[4] The number of possible combinations is further increased by the existence of various types of isomerism, for example, the Baker–Figgis isomers in the Keggin series (α, β, γ, δ, and ε).[5] In this context, the chemistry of the polyvacant heteropolytungstates offers great potential for the discovery of more and more finely tuned and specifically designed mixed-metal compounds. Among the Keggin derivatives, the borotungstate polyanions[6] represent a subclass of compounds with unusual properties as compared to the silicato and phosphato analogues.[7,8] Boron is an electron-deficient atom, which can adopt either trigonal or tetrahedral coordination modes.[9] The structure of the α-$[BW_{12}O_{40}]^{5-}$ Keggin anion reveals a central regular $\{BO_4\}$ unit,[10] in agreement with ^{11}B solid-state NMR data.[11] Formal removal of a $\{WO\}^{4+}$ group leads to the monovacant species $[HBW_{11}O_{39}]^{8-}$.[12] However, contrary to the well-established chemistry of the Si and P Keggin derivatives, acidification of the monovacant $[HBW_{11}O_{39}]^{8-}$ ion in the presence of tungstate ions does not lead directly to the saturated $[BW_{12}O_{40}]^{5-}$ ion. Previous studies by polarography and analytical ultracentrifugation have revealed the initial formation of a metastable compound with the formula α-$[H_3BW_{13}O_{46}]^{8-}$.[13] In unbuffered aqueous solution, this anion is slowly yet spontaneously converted to the thermodynamically stable α-$[BW_{12}O_{40}]^{5-}$ ion, while in strongly acidic media it condenses further leading to the tri-unit compound, which has been isolated and characterized in its acidic form of $H_{21}[B_3W_{39}O_{132}]\cdot 69\,H_2O$.[13] Despite these results, the chemistry and properties of the borotungstate ions remain unclear, and the interconversion scheme between these species has yet to be delineated. We report herein some new insights into borotungstate chemistry with the synthesis and characterization of two new borotungstate species, the monomeric anion α-$[H_3BW_{14}O_{48}]^{6-}$ and the dimeric anion $[H_6B_2W_{26}O_{90}]^{12-}$. We also present a re-investigation of the single-crystal X-ray diffraction determination of the trimeric $[H_6B_3W_{39}O_{132}]^{15-}$ ion, allowing reconciliation of the high symmetry observed in the solid state (C_{3h}) with the lack of symmetry in solution indicated by the 39-line ^{183}W NMR spectrum recently reported by Maksimov et al.[14] The 1D ^{183}W NMR analysis of the $[H_6B_3W_{39}O_{132}]^{15-}$ ion has been supported by a 2D COSY ^{183}W NMR, allowing thirteen partial assignments. Finally, structural and ^{183}W NMR characterizations of the three compounds, that is, the monomer, dimer, and trimer, each based on the same structural building block, give indications about the properties of the $[H_3BW_{13}O_{46}]^{8-}$ ion, especially about its peculiar reactivity.

Results and Discussion

Molecular structures of the anions

$Cs_5(NH_4)_{0.94}[H_3BW_{14}O_{48}]_{0.94}[BW_{12}O_{40}]_{0.06}\cdot 10\,H_2O$ ($CsNH_4$-2): We begin this section by discussing the structural disorder of the molecular unit within the crystal, and then proceed to describe the anion $[H_3BW_{14}O_{48}]^{6-}$ (denoted as **2**).

The X-ray structure of **$CsNH_4$-2** reveals a disordered molecular unit incorporating about 6% of the $[BW_{12}O_{40}]^{5-}$ ion and about 94% of the $[H_3BW_{14}O_{48}]^{6-}$ ion, both being located at the same crystallographic site (Figure 1a; Table 1). The disordered molecular unit is based on the non-disordered $\{BW_{11}O_{39}\}^{9-}$ moiety with either a $\{W{=}O\}^{4+}$ group located in its vacancy (giving the $[BW_{12}O_{40}]^{4-}$ ion) or an outer $\{W_3O_9\}$ grafted core leading to the $\{BW_{14}O_{48}\}^{9-}$ ion (**2**). The tungsten atoms labeled W5 and W8, belonging to the outer tritungstic group, were refined with a statistical occupancy

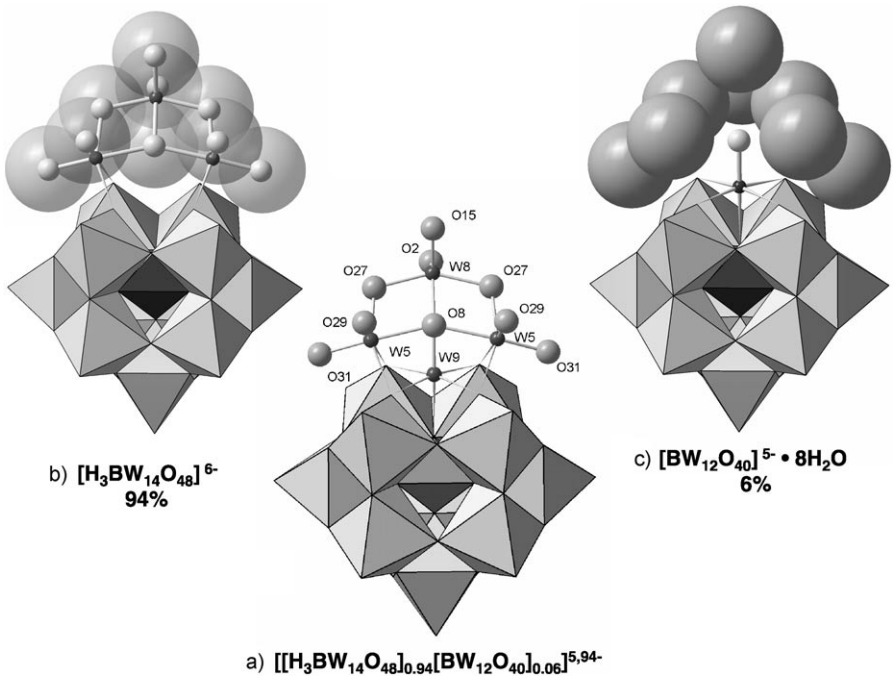

Figure 1. Structural representation of the molecular disorder in **$CsNH_4$-2** containing 94% $[H_3BW_{14}O_{46}]^{6-}$ ions and 6% $[BW_{12}O_{40}]^{5-}$ ions superimposed on the same crystallographic site. a) Molecular units consisting of a non-disordered monovacant $\{BW_{11}O_{39}\}^{9-}$ unit (polyhedral representation) capped by a disordered $\{W_4O_9\}$ core (ball-and-stick representation). b) Representation of the $[H_3BW_{14}O_{46}]^{6-}$ ion (**2**) showing the outer $\{W_3O_9\}$ core (with space-filling shown transparently) grafted onto the $\{BW_{11}O_{39}\}^{9-}$ unit. c) $[BW_{12}O_{40}]^{5-}$ ion surrounded by eight water molecules (space-filling model).

Table 1. Summary of crystal structure data.

	$CsNH_4$-2	**$CsNH_4$-3**	**NaH-4**
formula	$H_{26.58}Cs_5N_{0.94}BW_{13.88}O_{57.52}$	$H_{48}Cs_6N_6B_2W_{26}O_{102}$	$H_{156}Na_3B_3W_{39}O_{201}$
M [g mol^{-1}]	4187.48	7363.62	10644.80
T [K]	296(2)	296(2)	296(2)
crystal size [mm]	0.18×0.08×0.06	0.14×0.06×0.04	0.10×0.10×0.05
crystal system	orthorhombic	triclinic	hexagonal
space group	*Pnnm*	$P\bar{1}$	$P6_3/m$
a [Å]	18.4843(3)	12.7814(8)	21.7511(1)
b [Å]	19.6459(3)	18.746(2)	21.7511(1)
c [Å]	15.7813(2)	19.894(2)	21.6353(2)
α [°]	90	74.340(2)	90
β [°]	90	76.165(2)	90
γ [°]	90	89.887(2)	120
V [Å^3]	5730.9(2)	4446.2(5)	8864.6(1)
Z	4	2	2
ρ_{calcd} [g cm^{-3}]	4.853	5.500	3.988
$\mu(Mo_{K\alpha})$ [cm^{-1}]	30.975	36.029	25.323
$\lambda(Mo_{K\alpha})$ [Å]	0.71073	0.71073	0.71073
θ range [°]	1.51 to 27.50	1.10 to 27.5	1.08 to 27.49
data collected	36256	49838	55905
unique data	6825	20378	6971
unique data $I>2\sigma(I)$	5440	14759	4492
no. of parameters	386	1204	382
$R(F)$[a]	0.0514	0.0525	0.0754
$R_w(F^2)$[b]	0.1363	0.1405	0.2049
GOF	1.075	1.098	1.048

[a] $R_1=\frac{\sum||F_0|-|F_c||}{\sum|F_c|}$. [b] $R_w=\sqrt{\frac{\sum w(F_0^2-F_c^2)^2}{\sum w(F_0^2)^2}}$, $\frac{1}{w}=\sigma^2F_0^2+(aP)^2+bP$.

factor of 0.94, while a 0.06 complementary occupancy factor was found for the single W9 tungsten atom located in the vacancy. The nine outer oxygen atoms of the $\{W_3O_9\}$ core retain an occupancy factor of 1. In such a disordered scheme, these oxygen atoms, except for O8, could be either oxo or hydroxo ligands of the $\{W_3O_9\}$ core, or hydrating water molecules surrounding the $[BW_{12}O_{40}]^{5-}$ ion. These oxygen atoms, either oxo/hydroxo ligands or water molecules, interact with the cesium cations (Cs1, Cs2, Cs3, Cs4, and Cs5) with typical bond lengths (3.013(8)–3.524(8) Å). The O8 atom, which is common to both anions, corresponds to the terminal oxygen atom attached to W9 within $[BW_{12}O_{40}]^{5-}$, or the bridging oxygen between the two equivalent W5 atoms within the $\{W_3O_9\}$ outer capping core. Thus, in such an environment, the $[BW_{12}O_{40}]^{5-}$ ion is surrounded by eight water molecules, which confer to the overall structure, $\{[BW_{12}O_{40}]\cdot(H_2O)_8\}^{5-}$, a shape in space-filling volume similar to that observed for the $[H_3BW_{14}O_{48}]^{6-}$ ion (see Figure 1b and c). In this structural model, the charge balance of the disordered molecular unit is ensured by five non-disordered cesium cations and one ammonium cation, also refined with a 0.94 occupancy factor.

The structure of the $[BW_{14}O_{48}]^{9-}$ ion, shown in Figure 1b, consists of a $\{BW_{11}O_{39}\}^{9-}$ ion, capped by an outer tritungstic core, $\{W_3O_9\}$. Compound **$CsNH_4$-2** crystallises in the *Pnnm* space group, in which the $[BW_{14}O_{48}]^{9-}$ ion exhibits C_s molecular symmetry in the solid state. The $\{BW_{11}O_{39}\}^{9-}$ subunit is directly connected to two equivalent octahedra (W5 tungsten atoms) through four corner junctions. Both equivalent W5 atoms are mutually connected through the O8 oxygen atom, which ensures a corner junction. The third outer tungsten atom (W8) bears two *cis* terminal oxygen atoms and is bound to the two μ_2 O27 atoms and to the single μ_3 O8 atom. The W8 tungsten atom exhibits an unprecedented pentacoordinate arrangement, which makes compound **2** unique in the field of polyoxometalates. According to the elemental analysis, three protons are required for charge balance. Unfortunately, bond valence sum (BVS) calculations did not allow unambiguous location of the protonation sites. Nevertheless, the six terminal W–O bond distances within the outer $\{W_3O_9\}$ core fall in the range 1.724(11)–1.786(7) and their mean value is 1.763 Å, slightly larger than that observed in the $\{BW_{11}O_{39}\}^{9-}$ subunit (1.713 Å). The three protons are probably statistically distributed over these six terminal oxygen atoms. Selected bond distances within the $\{W_3O_9\}$ outer capping group are given in Table 2.

$Cs_6(NH_4)_6H_6B_2W_{26}O_{90}\cdot12H_2O$ ($CsNH_4$-3): The dimeric anion $[H_6B_2W_{26}O_{90}]^{12-}$ (**3**) is depicted in Figure 2. The structure consists of two $\{BW_{11}O_{39}\}^{9-}$ ions linked by a $\{W_4O_{12}\}$ core involving the W12, W13, W14, and W15 atoms. The central $\{W_4O_{12}\}$ linking group consists of four corner-connected octahedra with W-O-W angles of 150–157°. The arrangement of the outer $\{W_4O_{12}\}$ core reveals alternating long and short *trans* W–O bonds extending along the chain (see Table 2). For example, the short distance between the W(12) and O(40) atoms (1.710(15) Å) is consistent with W=O double-bond character, while the *trans* W(12)–O(43) bond is seen to be significantly longer (2.233(15) Å). The third *trans* W(13)–O(43) bond is short (1.704(13) Å), in agreement with W=O double-bond character, while the extended length of the remaining *trans* W(13)–O(46) bond

Table 2. Bond lengths [Å] within the outer Keggin groups for compounds **1**, **2**, and **3**.

$\{W_3O_9\}$ in **1**		$\{W_4O_{12}\}$ in **2**				$\{W_6O_{15}\}$ in **3**	
W5–O8	2.0983(19)	W12–O40	1.710(13)	W14–O47	1.694(12)	W7B–O25	2.241(11)
W5–O29	1.754(8)	W12–O41	1.752(15)	W14–O48	1.740(15)	W7B–O26	1.697(3)
W5–O31	1.786(7)	W12–O42	1.914(14)	W14–O45	1.930(13)	W7B–O22	1.842(7)
W5–O27	1.943(8)	W12–O24	1.983(13)	W14–O49	1.964(13)	W7B–O24#2	2.003(10)
W5–O22	1.958(6)	W12–O39	2.164(15)	W14–O50	2.208(12)	W7B–O24	1.840(11)
W5–O20	2.226(6)	W12–O43	2.235(13)	W14–O51	2.219(13)	W7B–O10	1.983(10)
W8–O27	1.958(7)	W13–O43	1.704(14)	W15–O52	1.724(13)	W7A–O25	1.677(11)
W8–O15	1.726(11)	W13–O44	1.737(14)	W15–O50	1.735(12)	W7A–O10	2.007(10)
W8–O2	1.774(13)	W13–O45	1.875(13)	W15–O42	1.878(14)	W7A–O22	1.878(8)
W8–O8	1.977(8)	W13–O28	1.937(14)	W15–O53	1.951(14)	W7A–O24	1.856(11)
		W13–O35	2.120(13)	W15–O54	2.148(15)	W7A–O24#2	1.967(10)
		W13–O46	2.271(14)	W15–O55	2.237(14)	W7A–O26	2.261(3)

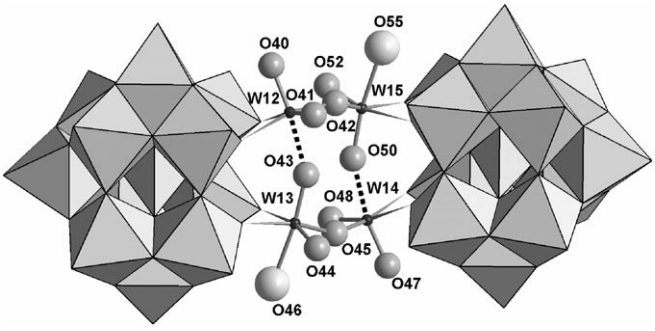

Figure 2. $[H_6B_2W_{26}O_{90}]^{12-}$ dimeric ion (**3**) showing the connections between two $\{BW_{11}O_{39}\}^{9-}$ units in polyhedral representation and the central $\{W_4O_{12}\}$ linking core (ball-and-stick). Large spheres correspond to the diprotonated oxygen atoms (aquo ligands) and the dark dotted lines represent the long W–O bonds within the O=W···W–OH_2 chains.

(2.270(12) Å) is characteristic of a terminal aquo ligand for O46. Alternating long and short W–O bonds running along the O=W···O=W–OH_2 chain are also observed within the second $\{W_2O_7\}$ fragment involving the W14 and W15 tungsten atoms. Such connectivity involving short and long alternating W–O bonds has been reported previously for the $[Si_2W_{23}O_{78}(OH)]^{9-}$ ion, which contains the same $\{W_2O_7\}$ core connecting two γ lacunary Keggin anions.[15] Interestingly, the two O=W···O=W–OH_2 chains within **3** are arranged in an anti-parallel fashion (head-to-tail), with the two water molecules O(46) and O(55) far from each other (see Figure 2). The coordination sphere of each tungsten atom within the central core is completed by an additional terminal oxygen atom. As in the case of **2**, elemental analysis requires the presence of six protons. Four of them belong to the two attached water molecules, while the remaining two should be statistically distributed over the four terminal oxygens, O(42), 0(44), O(48), and O(52), according to the W–O bond distances (1.723(17)–1.751(15) Å). Another structural feature is the cisoid arrangement of the two $\{BW_{11}O_{39}\}^{9-}$ moieties, as shown in Figure 3a. Such a cisoid configuration, associated with the antiparallel arrangement of the two O=W···O=W–OH_2 chains, results in the loss of any element of symmetry within the molecule. Alternatively, the dimer may be described in terms of the association of two chiral $\{H_3BW_{13}O_{46}\}^{8-}$ units, as shown in Figure 3b. Actually, the observed structure is built up from two enantiomerically equivalent $\{H_3BW_{13}O_{46}\}^{8-}$ units. The resulting molecular dimer remains chiral, but both enantiomers are present in the racemic crystal ($P\bar{1}$ centrosymmetric space group for **$CsNH_4$-3**).

$Na_3H_{18}B_3W_{39}O_{132}\cdot 56H_2O$ (NaH-4): Because the ^{183}W NMR spectrum of **4** cannot be fully understood on the basis of the reported solid-state structural data,[13,14] we decided to reconsider the structural determination of the anion **4**. The structure of the $[H_6B_3W_{39}O_{132}]^{15-}$ ion is shown in Figure 4.

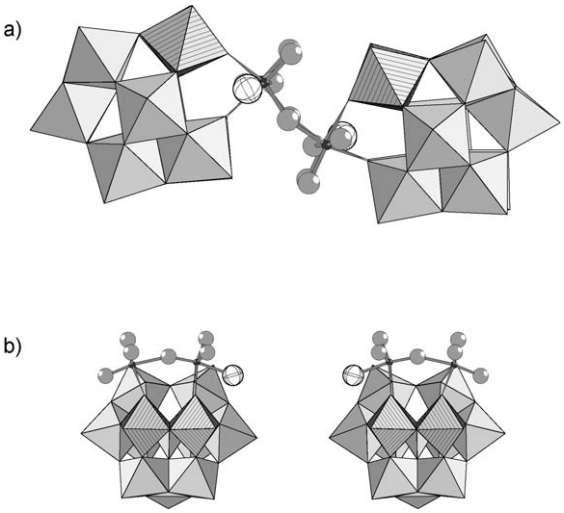

Figure 3. a) Top view of the anion **3** showing the cisoid arrangement of the two $\{BW_{11}O_{39}\}^{9-}$ subunits, highlighted by the relative positions of two hatched ditungstic groups (white ellipse = water molecule). b) Representation of the two enantiomers generated by the chiral $\{H_3BW_{13}O_{46}\}^{8-}$ moiety; anion **3** is built from two enantiomerically equivalent $\{H_3BW_{13}O_{46}\}^{8-}$ units.

NaH-4 crystallises in the hexagonal $P6_3/m$ space group, giving the highly symmetrical C_{3h} $\{H_6B_3W_{39}O_{132}\}$ motif. The general structural description is maintained and consists of three $\{BW_{13}O_{46}\}$ subunits, mutually linked by six corner-sharing octahedra. Actually, we found that a slight disorder, fundamental for the molecular symmetry, involves the six tungsten atoms within the central $\{W_6O_{15}\}$ core. These atoms appear equally distributed over two close positions, labeled A and B and separated by 0.565(2) Å (see Figure 4b). Such a disorder is rationalized by alternating long and short W–O bonds along the O=W···O=W–OH_2 chain, statistically oriented over two opposite directions (see Figure 4a). The positional disorder affects only the tungsten atoms, and not the

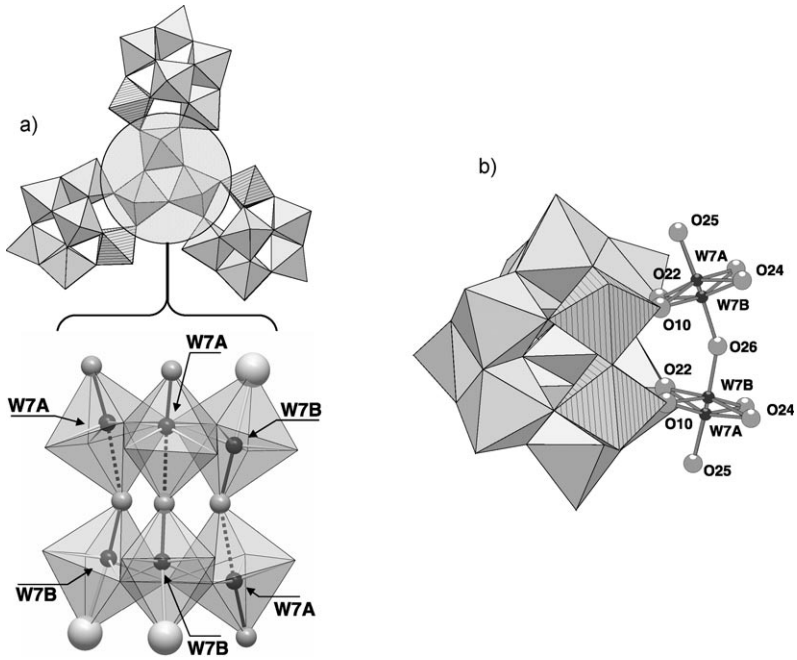

Figure 4. a) Top: polyhedral representation of the $[H_6B_3W_{39}O_{132}]^{15-}$ anion (**4**), the C_{3h} symmetry observed in the solid state is highlighted by the hatched ditungstic group within each $\{BW_{11}O_{39}\}^{9-}$ subunit. Bottom: expansion of the central $\{W_6O_{15}\}$ core, showing the distribution of the attached aquo ligands (large gray spheres) and the directions of the three O=W···O=W–OH_2 chains. b) Representation of the $\{BW_{13}O_{46}\}$ subunit in **4** (ball-and-stick) showing the disordered $\{W_2O_7\}$ group grafted onto the $\{BW_{11}O_{39}\}^{9-}$ moiety (polyhedral model).

oxygen atoms involved in the coordination of the disordered tungsten atoms. The O25 atom corresponds to an aquo ligand when bound to W7B and to a doubly-bonded oxo ligand when bound to W7A. The resulting alternating short and long bond distances within the O=W7A···O=W7B–OH_2 chain are 1.676(11), 2.260(3), 1.696(3), and 2.240(11) Å, respectively (see Table 2). Thus, the $\{WO_6\}$ octahedra for atoms W7A and W7B are axially distorted, which is a common feature of W^{VI} atoms. From such considerations, three aquo ligands have to be postulated in the molecular formula of the anion $[H_6B_3W_{39}O_{132}]^{15-}$. Similar to the dimeric anion, $[H_6B_3W_{39}O_{132}]^{15-}$ may be viewed as a fusion of three $\{BW_{13}\}$ chiral subunits, but in contrast to the dimer, the three $\{BW_{13}\}$ subunits are mutually connected in transoid fashions. Accordingly, a statistical distribution of the three O=W···O=W–OH_2 chains within the central $\{W_6O_{15}\}$ linking group may formally generate two diastereoisomers. In the first one, the three outer terminal aquo ligands are located over the same face of the $\{W_6\}$ trigonal prism and, consequently, the three outer W=O groups are located over the opposite face. Such an arrangement has to be excluded because the resulting C_3 symmetry should produce thirteen ^{183}W NMR resonances, which would then be inconsistent with the experimental 39-line spectrum.[14] Conversely, the second diastereoisomer consists of a distribution of one oxo and two aquo ligands over one face and of one aquo and two oxo ligands over the opposite face (see Figure 4a). Such an anion is chiral, but the racemic crystal ($P6_3/m$ space group) contains both enantiomers, statistically distributed over the same highly symmetrical crystallographic site ($\bar{6}$) to give the observed local disorder. In the anion **4**, the three $\{BW_{13}\}$ subunits are therefore mutually connected by three different bridges, W7A-O24-W7A, W7A-O24-W7B, and W7B-O24-W7B, which display different angles of 152.6(5)°, 144.2(6)°, and 131.4(6)°, respectively.

^{183}W NMR characterization of $[H_6B_3W_{39}O_{132}]^{15-}$ (4): The 1D and 2D ^{183}W NMR spectra of **4** are shown in Figure 5 and Figure 6, respectively. NMR data are given in Table 3. As already reported by Maksimov et al.,[14] the ^{183}W NMR spectrum of **4** is remarkable in that it contains 37 resolved resonances over a large chemical shift range (between $\delta = -110$ and -400 ppm). The very sharp line at $\delta = -132.40$ ppm is assigned to the presence of a minor amount of $[BW_{12}O_{40}]^{5-}$ as an impurity, initially present at a level of less than 3%, but which slowly increases with ageing. Of the 36 remaining peaks, 33 exhibit the same intensity ratio, while three of them in the high-frequency region at $\delta = -129.1$, -122.9, and -119.7 ppm appear to be accidentally degenerate (relative intensity of 2).[16] Therefore, the ^{183}W NMR spectrum can be interpreted as a 39-line spectrum. This feature is related to the lack of any symmetry of the $[H_6B_3W_{39}O_{132}]^{15-}$ anion, as discussed above. Obviously, a complete assignment of these resonances to the 39 tungsten nuclei cannot be established. Nevertheless, partial assignments may be proposed on the basis of tungsten–tungsten connectivity by means of a 2D COSY experiment (Figure 6a and b). In favorable cases, that is, sharp and well-resolved resonances, ^{183}W 2D NMR correlation spectroscopy (COSY[17] or INADEQUATE[18]) has been successfully applied to establish structures of polyoxometalates and to assign all of the tungsten resonances of the anion, even for chiral polyoxometalates.[19] A striking feature of the spectrum is the presence of strongly low-frequency shifted resonances, specifically two isolated sets of three resonances near $\delta = -400$ and -250 ppm; the remaining resonances, observed as five separated sets of 3W (-207 to -213), 9W (-188 to -170), 3W (-160 to -152), 6W (-150 to -135), and 12W (-135 to -115 ppm), fall in the usual range observed for Keggin derivatives.[20] As suggested by Maksimov et al., such peculiar low-frequency resonances could be related to the unusual arrangement of the six central W atoms. While the W atoms of the $\{BW_{11}\}$ moiety share four μ_2-O

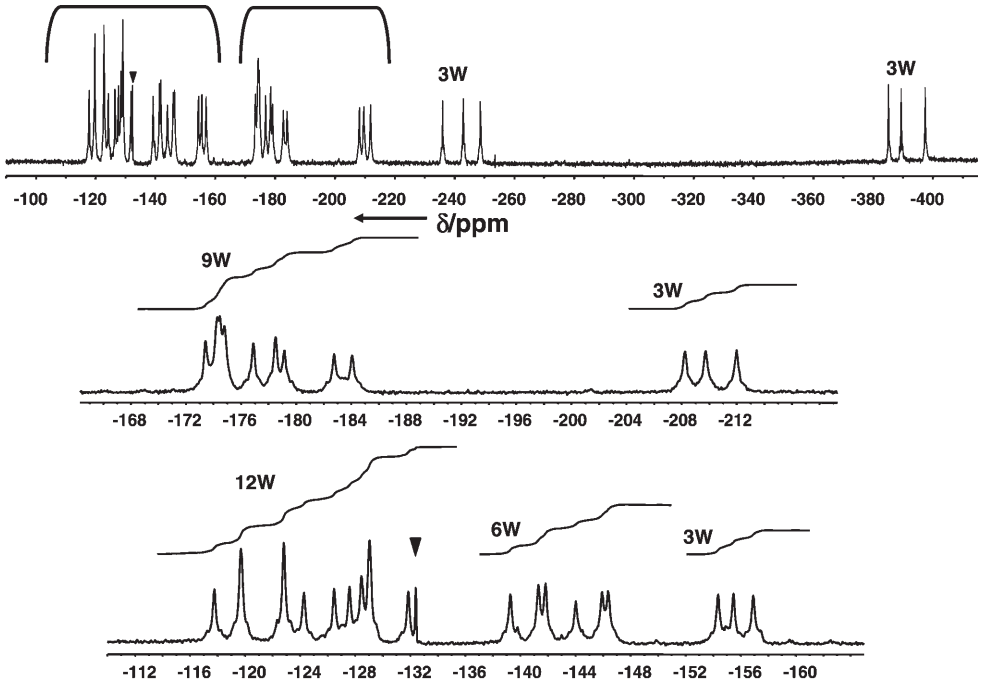

Figure 5. ^{183}W 1D NMR spectrum of the $[H_6B_3W_{39}O_{132}]^{15-}$ ion with expanded spectral regions (▼ = $[BW_{12}O_{40}]^{5-}$ impurity).

atoms, distributed as two edge and two corner junctions, each of these six central W is connected to five neighboring W exclusively through corner junctions. In addition, three of them, that is, W7B, adopt a peculiar arrangement. They are bound to a terminal aquo ligand, while in the *trans* position the oxygen atom O26 interacts smoothly through a long bond (2.260(3) Å) with the adjacent W7A atom. Consequently, the W7B atoms have no "true" terminal oxo ligand in their coordination sphere and such a situation could be invoked as a qualitative explanation for the pronounced shielding of these nuclei. Theoretical studies based on Hückel molecular orbital (EHMO)[21] or effective core DFT calculations[22] have established a relationship between the ^{183}W chemical shift and the atomic charge on the tungsten atom and indicate that increasing positive charge on the metal results in a shielding of the nucleus. pπ–dπ interactions with the oxygen atom orbitals contribute to the shielding of the W nucleus. Such interactions are strong with the terminal oxygen atom, leading to double-bond character, and to a lesser extent with the bridging oxygen atoms. There are few reported examples of tungsten atoms with such coordination schemes, that is, no true terminal oxygen atom and four equatorial corner junctions. The ^{183}W NMR spectrum of $[HSi_2W_{23}O_{78}]^{9-}$ features a peculiar signal at very low frequency ($\delta = -300$ ppm) related to the presence of a {O=WA···O=WB–OH} chain,[15] similar to that described for **4**. In such an arrangement, the pseudo terminal O atom attached to WB [(WB–O) = 1.72(1) Å] interacts smoothly with WA [(WA···O) = 2.31(1) Å]. Another example showing the influence of the number of equatorial corner junctions on the chemical shift is found in the large Preyssler anion, $[NaP_5W_{30}O_{110}]^{14-}$, which exhibits four resonances, all of them in the low-frequency region.[23] The most shifted signals at $\delta = -288$ and -275 ppm, assigned on the basis of their intensity ratio, correspond to equatorial W atoms that share only corner junctions with their four equatorial W neighbours, whereas the other two resonances at $\delta = -208$ and -209 ppm correspond to W atoms that share one edge and three corner junctions.[24] As a consistent extension of such considerations, a further increase in the number of edge junctions around the tungsten atom results in a significant deshielding, as observed for $[BW_{12}O_{40}]^{5-}$ (two edges and two corners; $\delta = -133.5$ ppm)[25] and for the Lindqvist ion, $[W_6O_{19}]^{2-}$ (only edges; $\delta = +58.9$ ppm).[26] The relationship between the types of junctions and the W shielding was first proposed and justified theoretically by Kazansky et al.[27] In summary, the magnitude of the ^{183}W shielding in a {WO_6} environment increases: i) with increasing involvement of the terminal O atoms in outer interactions, ii) with increasing number of equatorial corner junctions. In the $[H_6B_3W_{39}O_{132}]^{15-}$ ion, the W7B atoms with attached terminal aquo ligands atoms show both features, that is, four corner junctions in their equatorial planes and no "true" terminal oxygen atom. Thus, on the basis of above considerations, these W7B atoms should be responsible for the set of three resonances at $\delta = -400$ ppm. From this first assignment, 2D COSY ^{183}W NMR allows other partial assignments, as presented in Table 3. The lack of symmetry requires unambiguous identification of the 39 W to complete the labelling of the W atoms. Keeping the labels used for X-ray diffraction analysis, the three {BW_{13}} subunits may be distinguished by *a*, *b*, and *b*′ sub-labels, as shown in Figure 7. The *a* moiety has its outer W7A=O directed towards a face of the central {W_6} core, while the *b* and *b*′ subunits are both directed to-

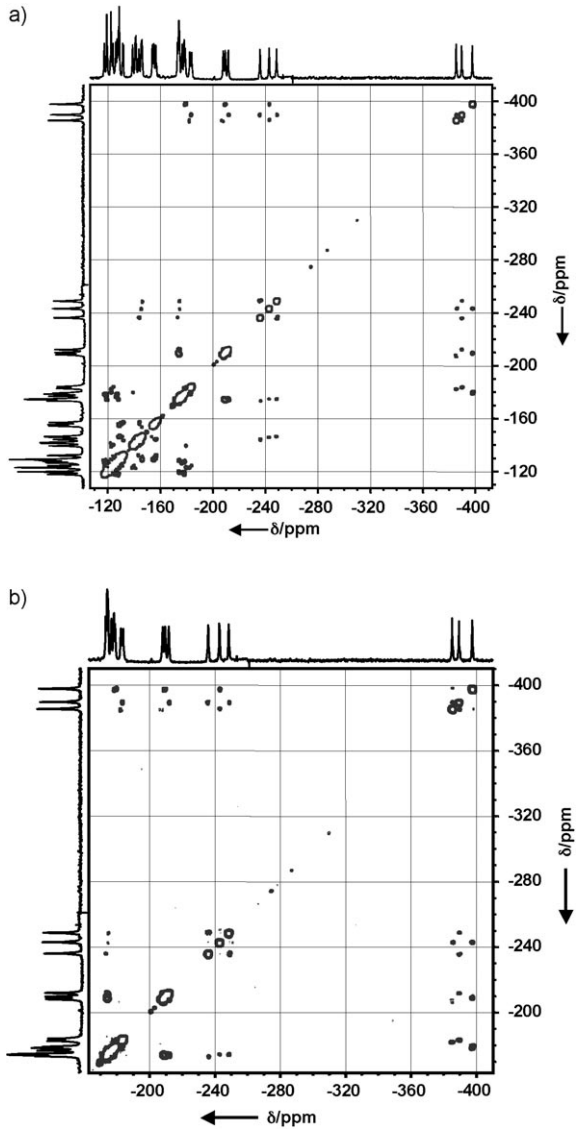

Figure 6. 2D COSY ^{183}W NMR spectrum of **4**: a) full spectrum; b) expansion of the −150/−400 ppm region.

wards W7B−OH_2. The opposite face contains the W7B−OH_2 of the *a*-{BW_{13}} subunit and the two W7A=O of both *b*- and *b*′-{BW_{13}}. In addition, the tungsten atoms have to be labeled A and B to distinguish those distributed on either side of the crystallographic plane (see Figure 7b). The A-labeled atoms within a {BW_{13}} subunit are located on the same side of the W7A central atom and the B-labeled atoms are distributed towards W7B. Then, except for the in-plane atoms W1*z*, each tungsten atom may be identified by the notation WXY*z*, where X = 2 to 7, Y = A or B, and *z* = *a*, *b* or *b*′. As discussed above, the three low-frequency resonances are assigned to the three W7B*z* atoms. According to the 2D COSY data (see Figure 6 and Table 4), these three lines are correlated to three groups of three close resonances {−248.7/−243.0/−236.1}, {−212.0/−209.7/−208.2}, and {−184.1/−182.8/−179.2}. This corresponds to $^{2}J_{W\text{-}O\text{-}W}$ couplings[28] of W7B*z* atoms with W7A*z* atoms of the {W_6} central core, and with W3B*z* and W6B*z* atoms belonging to the {BW_{11}} subunits. The signal at $\delta = -389.4$ ppm is correlated to those at both $\delta = -248.7$ and -236.1 ppm and, similarly, the signal at $\delta = -243.0$ ppm is correlated to those at both $\delta = -397.5$ and -385.2 ppm. This coupling scheme is consistent with the four corner junctions within the {W_6} central core, involving W7B*a* connected to W7A*b* and W7A*b*′ and W7A*a* connected to W7B*b* and W7B*b*′. The set of three resonances at around $\delta = -240$ ppm can therefore be assigned to the W7A*z* atoms within the {W_6} core. This assignment for W7A*z* is consistent with the four equatorial corner junctions of these atoms (see above). In addition, cross-peaks observed for the $\delta = -397.5$ and -385.2 ppm lines on the one hand, and for the $\delta = -248.7$ and -236.1 ppm lines on the other hand, are consistent with the corner junctions between adjacent W7B*b* and W7B*b*′ or W7A*b* and W7A*b*′. In summary, the signals at $\delta = -389.4$ and -243.0 ppm can only be assigned to W7B*a* and W7A*a*, respectively. Discrimination between the tungsten atoms belonging to the *b* or *b*′ subunit is precluded because the W7A*b* and W7A*b*′ atoms exhibit exactly the same coupling patterns with the initially assigned W7A*a* atoms. The same holds for W7B*b* and W7B*b*′ with respect to W7B*a*. Other partial assignments can be attempted, since correlations between the {W_6} core and W3Y*z* and W6Y*z*, belonging to the three *a*-, *b*-, and *b*′-{BW_{11}} subunits, are clearly observed. The W7B*z* atoms are connected to the {$\delta = -212.0/-209.7/-208.2$ ppm} and {$\delta = -184.1/-182.8/-179.2$ ppm} ensembles, while the W7A*z* atoms are connected to those at ($\delta = -174.5/-174.3/-173.4$ ppm) and ($\delta = -146.4/-146.0/-144.0$ ppm). Among these four ensembles, the two groups {$\delta = -212.0/-209.7/-208.2$ ppm} and {$\delta = -174.5/-174.3/-173.4$ ppm) are mutually correlated through large off-diagonal peaks, which originate from the corner junctions between W3A*z* and W3B*z*. This assignment is reinforced by the lack of any other correlations between the remaining W6A*z* and W6B*z* groups, consistent with edge junctions between these atoms.[29] The three resonances {$\delta = -212.0/-209.7/-208.2$ ppm} are thus attributed to the three W3Bz (z = *a*, *b*, and *b*′) and those at {$\delta = -174.5/-174.3/-173.4$ ppm} to the three W3A*z* atoms. The remaining groups, at {$\delta = -184.1/-182.8/-179.2$ ppm} and at {$\delta = -146.4/-146.0/-144.0$ ppm}, can then be attributed to W6B*z* and W6A*z*, respectively. Eighteen lines have been partially assigned to the W7Y*z*, W3Y*z*, and W6Y*z* tungsten atoms, corresponding to the six central W atoms and to the twelve W belonging to the Keggin subunits, lining the lacuna. The assignments of the W7B*a* and W7A*a* atoms therefore permit assignment of the $\delta = -212.0$, -184.1, -174.3, and -145.9 ppm lines to the correlated W3B*a*, W6B*a*, W3A*a*, and W6A*a* atoms, respectively (see Table 3). Further partial assignments can be attempted from the connectivity of the W6Y*z* and W3Y*z* atoms, but the close chemical shifts of the correlated peaks and the lack of any correlations through weak edge couplings allow only: i) assignment of the groups of three close resonances to the different ensembles of three tungsten atoms {WXA*a*/WXA*b*/WXA*b*′} and {WXB*a*/WXB*b*/WXB*b*′}, denoted as

Table 3. ^{183}W NMR data for $[H_6B_3W_{39}O_{132}]^{15-}$.[a]

Relative integral	δ [ppm]	$\bar{\delta}$ [ppm]	Assignment	Remarks
3 W	−397.5 −389.4 −385.2	−390.7	W7Bz ($Z=b$ or b') W7Ba W7Bz ($z=b$ or b')	no true terminal oxygen atoms; four corner junctions; {W6} central core
3 W	−248.7 −243.0 −236.1	−242.6	W7Az ($z=b$ or b') W7Aa W7Az ($z=b$ or b')	four corner junctions; {W6} central core
3 W	−212.0 −209.7 −208.2	−210.0	W3Ba W3Bz ($z=b$ or b') W3Bz ($z=b$ or b')	W atoms lining the lacuna of $\{BW_{11}\}$
	−184.1 −182.8 −179.2	−182.0	W6Ba W6Bz ($z=b$ or b') W6Bz ($z=b$ or b')	
9 W	−178.5 −176.9 −174.8	−176.7	W1z ($z=a$, b or b')	
	−174.5 −174.3 −173.4	−174.1	W3Az ($z=b$ or b') W3Aa WAz ($z=b$ or b')	W atoms lining the lacuna of $\{BW_{11}\}$
3 W	−156.9 −155.5 −154.4	−155.6	W2Az or W5Az ($z=a$, b or b')	
	−146.4 −145.9 −144.0	−145.4	W6Az ($z=b$ or b') W6Aa W6Az ($z=b$ or b')	W atoms lining the lacuna of $\{BW_{11}\}$
6 W	−141.8 −141.3 −139.3	−140.8	W2Bz or W5Bz ($z=a$, b or b')	
*	−132.4			$[BW_{12}O_{40}]^{5-}$ (impurity)
6 W	−131.9 −129.1(×2)	−130.0	W2Az or W5Az ($z=a$, b or b')	
6 W	−128.5 −127.6 −126.5	−127.5	W4Az or W4Bz ($z=a$, b or b')	
6 W	−124.3 −122.8(×2)	−123.5	W5Az or W5Bz ($z=a$, b or b')	
	−119.7(×2) −117.8	−119.1	W4Az or W4Bz ($z=a$, b or b')	

[a] Mean value of the three chemical shifts of each triad.

WXA and WXB triads, respectively; ii) the proposal of some partial assignments, because some ambiguities remain. The results of the assignments made with the aid of the ^{183}W COSY spectrum are summarized in Table 3. The connectivity matrix (experimental and theoretical) based on $^2J_{W\text{-}O\text{-}W}$ corner couplings between the eleven triads within the $\{BW_{11}O_{39}\}$ subunit is shown in Table 4. The expanded 2D COSY spectrum, showing the complete correlation pathway, is given in the Supporting Information (Figures S1 a–c). According to their remaining connections, no other cross-peaks are observed for either the W3Az or W3Bz triads. On the other hand, each triad, W6A and W6B, exhibits two different cross-correlations related to the corner junctions W6Y–W2Y and W6Y–W5Y (Y = A or B). From these observations, the {$\delta=-131.9/-129.1(\times2)$ ppm} and {$\delta=-156.9/-155.9/-154.4$ ppm} groups are assigned to the W2A or W5A triads and the {$\delta=-141.8/-141.3/-139.3$ ppm} or {$\delta=-124.3/-112.8(\times2)$ ppm} triads are assigned to the W2B or W5B triads. However, these assignments must remain partial because the lack of any edge correlation precludes assignment of these ensembles to the W2Y or W5Y triads, respectively. The remaining triads, W4A, W4B, and W1, are also mutually corner-connected according to the observed cross-correlations between the {$\delta=-178.5/-176.9/-174.8$ ppm}, {$\delta=-119.7(\times2)/-117.8$ ppm}, and {$\delta=-128.5/-127.6/-126.5$ ppm} ensembles. The two groups at {$\delta=-119.7(\times2)/-117.8$ ppm} and {$\delta=-128.5/-127.6/-126.5$ ppm} exhibit close chemical shift values ($|\Delta\bar{\delta}|=8.4$ ppm), most probably due to the four-bond remoteness of the W4A and W4B triads starting from the origin of the dissymmetry within the anion, that is, the $\{W_6\}$ central core. Finally, the remaining isolated set of resonances {$\delta=-178.5/-176.9/-174.8$ ppm} is attributed to the W1 triad.

IR spectroscopy: The IR spectra of **Cs-1**, **$CsNH_4$-2**, **$CsNH_4$-3**, and **Cs-4** (shown in the Supporting Information, Figure S2) differ significantly from that of the monovacant precursor $K_8[HBW_{11}O_{39}]\cdot10H_2O$. The ν(W-O-W) stretching mode gives absorptions in the range from 850 to 650 cm^{-1}. Direct connections between the grafted cores $\{W_2O_7\}$ within multi-unit compounds give rise to strong characteristic absorptions at 726 cm^{-1} and 799 cm^{-1} for the dimer (**$CsNH_4$-3**) and the trimer (**CsH-4**), respectively.

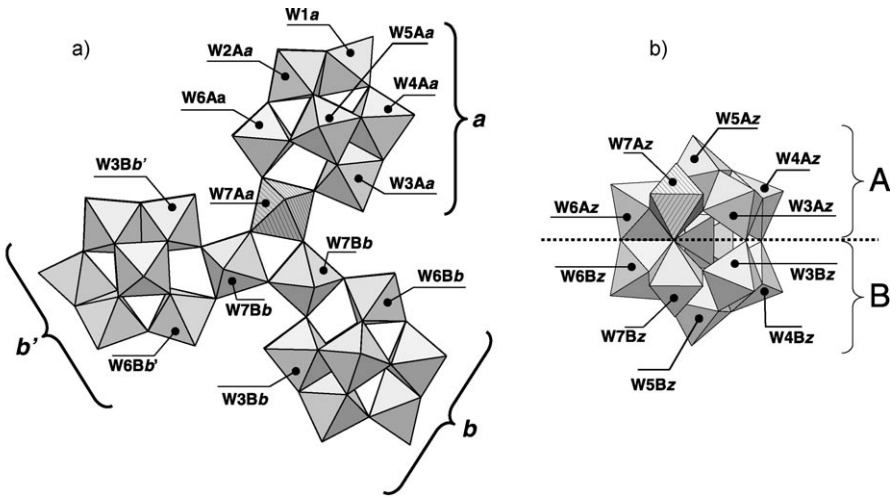

Figure 7. Tungsten atom-labeling scheme in the chiral $[H_6B_3W_{39}O_{132}]^{15-}$ anion. a) The three $\{BW_{13}\}$ subunits are labelled *a*, *b*, and *b'*; b) each of them is divided into two halves, A and B, with respect to the crystallographic plane, providing WXYz labels with X = 2 to 7, Y = A or B, and z = *a*, *b* or *b'* (except for the in-plane W1z atom).

Synthesis and properties in solution: Tézé et al. have reported on the addition of tungstate to the monovacant $[HBW_{11}O_{39}]^{8-}$ ion. They evidenced the $\{BW_{13}O_{46}\}$ species in solution by polarography and ultracentrifugation but without any structural characterization, for example, by ^{183}W NMR or single-crystal X-ray diffraction analysis. Nevertheless, the three $\{BW_{13}\}$-containing anions, derived as the monomer (**2**), dimer (**3**), and trimer (**4**), constitute probes for the structural relationship between these species. The condensation of tungstate ions onto the $[HBW_{11}O_{39}]^{8-}$ ion in acetate buffer can be monitored by polarography. As the amount of added $[WO_4]^{2-}$ ions is increased, the first reduction wave of the $[HBW_{11}O_{39}]^{8-}$ ions, observed at $E_{1/2} = -0.81$ V versus Ag/AgCl, gradually decreases at the expense of a new electron exchange at -0.52 V versus Ag/AgCl. The limiting diffusion currents for both exchanges versus the {W}/{BW_{11}} ratio are shown graphically in Figure 8 and clearly evidence a slope breaking for two equivalents of added tungstate ions, in agreement with the findings of Tézé et al.[13] Under such conditions, no other compound is evidenced for higher {W}/{BW_{11}} ratios, and the $\{BW_{13}\}$ anion formed appears to be indefinitely stable under the polarographic conditions (about 10^{-3} mol L^{-1} in 1 mol L^{-1} sodium acetate buffer). A pH-metric titration with hydrochloric acid was carried out on a mixture containing $[HBW_{11}O_{39}]^{8-}$ and $[WO_4]^{2-}$ in a 1:2 ratio. The curve (Supporting Information,

Table 4. Part of the connectivity matrix ({BW_{11}} moiety) of $[H_6B_3W_{39}O_{132}]^{15-}$, including on the diagonal the mean experimental δ values.[a]

	W1*z*	W2A	W2B*z*	W3A*z*	W3B*z*	W4A*z*	W4B*z*	W5A*z*	W5B*z*	W6A*z*	W6B*z*
W1z	−176.7	(edge)	(edge)			**corner**	**corner**				
W2Az	(edge)	−155.6 or −130.0	(edge)					**corner**		**corner**	
W2Bz	(edge)	(edge)	−140.8 or −123.5						**corner**		**corner**
W3Az				−174.1	**corner**	(edge)		(edge)			
W3Bz				**corner**	−210.0		(edge)		(edge)		
W4Az	**corner**			(edge)		−127.5 or −119.1	**corner**	(edge)			
W4Bz	**corner**				(edge)	**corner**	−127.5 or −119.1		(edge)		
W5Az		**corner**		(edge)		(edge)		−155.6 or −130.0		**corner**	
W5Bz			**corner**		(edge)		(edge)		−140.8 or −123.5		**corner**
W6Az		**corner**						**corner**		−145.4	(edge)
W6Bz			**corner**						**corner**	(edge)	−182.0

[a] Bold = observed corner coupling; in brackets = unobserved edge coupling.

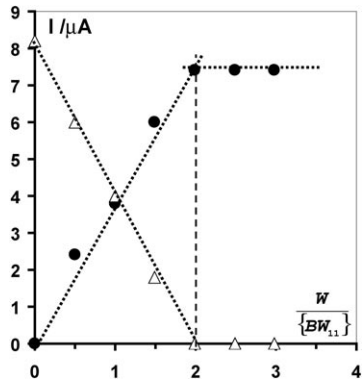

Figure 8. Limiting diffusion currents versus W/{BW_{11}} ratio of $E_{1/2}=-0.81$ V (Ag/AgCl) (△, $[HBW_{11}O_{39}]^{8-}$) and $E_{1/2}=-0.52$ V (Ag/AgCl) (●, $[H_3BW_{13}O_{46}]^{7-}$).

Figure S3) shows a first pH jump for about 4.5 equivalents of protons and a second, less well defined one, for about 6–8 equivalents of protons. These results can be interpreted in terms of successive acidobasic processes occurring in a narrow pH range, which consist of i) the acidic condensation of tungstate onto the $[HBW_{11}O_{39}]^{8-}$ ions according to Equation (1),

$$[HBW_{11}O_{39}]^{8-} + 2\,WO_4^{2-} + 4\,H^+ \rightleftharpoons [H_3BW_{13}O_{46}]^{8-} + H_2O \quad (1)$$

consistent with the polarographic results, ii) protonation of the resulting $[H_3BW_{13}O_{46}]^{8-}$ ion according to Equation (2), and iii) the dimerization process according to Equation (3),

$$[H_3BW_{13}O_{46}]^{8-} + H^+ \rightleftharpoons [H_4BW_{13}O_{46}]^{7-} \quad (2)$$

$$2\,[H_4BW_{13}O_{46}]^{7-} + 2\,H^+ \rightleftharpoons [H_6B_2W_{26}O_{90}]^{12-} + 2\,H_2O \quad (3)$$

which occurs below pH 3. In the light of these results, the $[H_4BW_{13}O_{46}]^{7-}$ ion was prepared in acetate buffer at about pH 4.8. Elemental analysis of the isolated cesium salt was consistent with the expected 1:13 ratio of B to W. Seven cesium ions per anion were found, consistent with −7 for the anionic charge and four attached protons. Thus, on the basis of the structural characterizations of the anions **2**, **3**, and **4**, the formula $[H_4BW_{13}O_{46}]^{7-}$ could be proposed, the protons most probably being distributed over the six terminal oxygen atoms as an aquo and two hydroxo groups within the {W_2O_7} outer cap. However, various attempts to obtain single crystals containing the $[H_4BW_{13}O_{46}]^{7-}$ ion failed. In aqueous ammonium chloride solution, crystals resulting from the *syn*-crystallization of the $[H_3BW_{14}O_{48}]^{6-}$ and α-$[BW_{12}O_{40}]^{5-}$ ions were obtained. This result indicates that the $[H_4BW_{13}O_{46}]^{7-}$ anion is unstable in unbuffered medium and is slowly transformed into $[BW_{12}O_{40}]^{5-}$ and $[H_3BW_{14}O_{48}]^{6-}$ according to Equation (4).

$$2\,[H_4BW_{13}O_{46}]^{7-} + 3\,H^+ \rightleftharpoons [BW_{12}O_{40}]^{5-} + [H_3BW_{14}O_{48}]^{6-} + 4\,H_2O \quad (4)$$

Various attempts to characterise the $[H_4BW_{13}O_{46}]^{7-}$ ion by ^{183}W NMR in solution resulted in complex spectra characteristic of mixtures of several species, always containing the α-$[BW_{12}O_{40}]^{5-}$ anion (single sharp resonance at $\delta\approx -132.5$ ppm) (Supporting Information, Figure S4). The $[H_3BW_{14}O_{48}]^{6-}$ ion exhibits similar behavior and gives a ^{183}W NMR spectrum characteristic of an equilibrium involving several species, such as isopolytungstates ($\delta=59.4$ and 50.8 ppm) (Supporting Information, Figure S5). In more acidic solution, at pH in the range 2–3, the $[H_4BW_{13}O_{46}]^{7-}$ anion undergoes self-condensation to give the $[H_6B_2W_{26}O_{90}]^{12-}$ dimeric anion (**3**) according to Equilibrium (3). However, the dimeric compound is also unstable in this pH range and is spontaneously converted into the $[BW_{12}O_{40}]^{5-}$ anion and by-products, as shown by the ^{183}W NMR spectrum (Supporting Information, Figure S6). Finally, the condensation process is achieved in strongly acidic medium (about 1 mol L^{-1} in sulfuric acid)[13] and leads to the formation of the ultimate condensed species $[H_6B_3W_{39}O_{132}]^{15-}$, isolated and morphologically described as hexagonal borotungstic acid about a century ago.[30] Alkalimetric titration of the mixed salt $Na_3H_{18}[B_3W_{39}O_{132}]\cdot 56\,H_2O$ (**NaH-4**) in aqueous solution shows a first pH jump corresponding to the simultaneous neutralization of twelve protons (Supporting Information, Figure S7). A second step is clearly observed corresponding to the exchange of three additional protons at pH 5.5 ($pK_a\approx 4.5$). Above pH 7, no further pH jump is observed. Thus, among the eighteen protons, twelve are strongly acidic and three correspond to weak acidities ($pK_a\approx 4.5$). The acidities of the three remaining attached protons are too low to be observed before hydrolysis of the compound (pH > 7). The results are fully consistent with the presence of three aquo ligands, corresponding to six weakly acidic protons.

Conclusion

New insight into the borotungstate system has been gained. Two novel molecular structures, each based on the $[H_3BW_{13}O_{46}]^{8-}$ precursor have been described, and the origin of the lack of symmetry within the trimeric $[H_6B_3W_{39}O_{132}]^{15-}$ anion has been elucidated through X-ray structural reinvestigation supported by 1D and 2D COSY ^{183}W NMR. The origin of the strong shielding of the central tungsten atoms ($\delta\approx -400$ and -250 ppm) has been discussed in relation to the geometrical peculiarities of these atoms. Breaking the C_{3h} symmetry within the $[H_6B_3W_{39}O_{132}]^{15-}$ ions gives rise to 39 resonances, distributed over thirteen groups of three lines. Moreover, detailed analysis of the 2D COSY spectrum permits the assignment of the 13 groups of resonances to the overall tungstic triads. The formation of the three species **2**, **3**, and **4** is mainly con-

trolled by pH. A notably rare pentacoordinated arrangement for a W^{VI} atom is observed within $[H_3BW_{14}O_{48}]^{6-}$, revealing the remarkable complexing ability of the $[H_3BW_{13}O_{46}]^{8-}$ precursor, which appears to represent a good candidate for the formation of novel mixed-metal compounds. Moreover, the most striking property of the $[H_3BW_{13}O_{46}]^{8-}$ anion is its ability to produce chiral multiunit compounds, that is, $[H_6B_2W_{26}O_{90}]^{12-}$ and $[H_6B_3W_{39}O_{132}]^{15-}$. The structure of the monomeric precursor, deduced from its dimeric and trimeric forms, most likely arises from grafting of the $\{O{=}W{\cdots}W{-}OH_2\}$ core onto the $[HBW_{11}O_{39}]^{8-}$ moiety. This anion, which is therefore chiral, should be a good candidate for chiral POM synthesis under conditions of chiral induction (for the synthesis of non-racemic mixtures).[31]

Experimental Section

Preparation of the compounds: All chemicals were reagent grade, and were purchased from commercial sources and used without further purification. The precursor $K_8HBW_{11}O_{39}\cdot 13H_2O$ and the anion $[H_6B_3W_{39}O_{132}]^{15-}$ (**4**) were synthesized according to reported procedures.[13] According to analysis by proton titration, thermogravimetry, elemental analysis, and X-ray diffraction, three sodium cations per anion were found, giving the formula as $H_{18}Na_3[B_3W_{39}O_{132}]\cdot 56H_2O$.

$Cs_7H_4BW_{13}O_{46}\cdot 11H_2O$ (Cs-1): $K_8\alpha$-$HBW_{11}O_{39}\cdot 13H_2O$ (10 g, 3 mmol) was suspended in 150 mL of sodium acetate/acetic acid buffer (pH 4.8; 1 mol L^{-1}). 1 mol L^{-1} Na_2WO_4 solution (6 mL) was then added, instantaneously clarifying the cloudy starting solution. After 15 min, cesium chloride (10 g, 60 mmol) was slowly added until an oily colorless residue was deposited. After 1 h, the solution was decanted from the beaker and the sticky oily phase was treated with ethanol until a white powder was obtained, which was collected by filtration and dried by rinsing with diethyl ether. Yield: 12 g (≈93%). IR (KBr): $\tilde{\nu}$ = 1000(w), 949(m), 891(m), 846(m), 821(m), 771(m), 719(w), 648(w), 523(m), 348 cm^{-1} (m); elemental analysis calcd (%) for $H_{26}Cs_7BW_{13}O_{57}$: Cs 21.8, B 0.23, W 55.98; found: Cs 22.57, B 0.25, W 56.60.

$Cs_5(NH_4)_{0.94}[H_3BW_{14}O_{48}]_{0.94}[BW_{12}O_{40}]_{0.06}\cdot 10H_2O$ ($CsNH_4$-2): $Cs_7H_4BW_{13}O_{46}\cdot 11H_2O$ (1 g, 0.233 mmol) was dissolved in 1 mol L^{-1} aqueous ammonium chloride solution (20 mL). The solution was left to stand in an open vessel for crystallization. After three days, well-shaped colorless parallelepipedic crystals, suitable for X-ray diffraction analysis, were collected. Yield: 0.32 g (35%). The stoichiometry of the compound **$CsNH_4$-2** was inferred from X-ray structural data. IR (KBr): $\tilde{\nu}$ = 997(w), 950(m), 852(w), 823(m), 773(m), 722(m), 648(w), 521(m), 381(m), 364(w), 350(vw), 228 cm^{-1} (vw); elemental analysis calcd (%) for $H_{26.58}Cs_5N_{0.94}BW_{13.88}O_{57.52}$: Cs 16.85, N 1.10, B 0.25, W 60.10; found: Cs 16.87, N 1.50, B 0.25, W 61.44.

$Cs_6(NH_4)_6H_6B_2W_{26}O_{90}\cdot 12H_2O$ ($CsNH_4$-3): $K_8HBW_{11}O_{39}\cdot 13H_2O$ (10 g, 3 mmol) was suspended in water (60 mL). Then, 1 mol L^{-1} Na_2WO_4 solution (6 mL) and 4 mol L^{-1} hydrochloric acid solution (ca. 5 mL) were added until pH 2.5 was attained. After 30 min, cesium chloride (1.6 g, 9.5 mmol) was added, leading to the precipitation of a white solid. The crude product was collected by filtration, washed with ethanol, and dried by rinsing with diethyl ether. The solid (5.0 g) was dissolved in 1 mol L^{-1} ammonium chloride solution (100 mL) under moderate heating (40 °C). The cloudy solution was filtered and allowed to stand for crystallization. After two days, well-shaped colorless parallelepipedic crystals, suitable for X-ray diffraction analysis, were collected. Yield: 2.5 g (≈50%). IR (KBr): $\tilde{\nu}$ = 999(w), 956(m), 898(m), 853(w), 828(m), 726(m), 632(m), 518(w), 374(m), 337 cm^{-1} (m); elemental analysis calcd (%) for $H_{54}Cs_6N_6B_2W_{26}O_{102}$: Cs 10.83, N 1.46, B 0.29, W 64.91; found: Cs 10.89, N 1.21, B 0.25, W 65.71.

$Cs_{15}H_6B_3W_{39}O_{132}\cdot 15H_2O$ (CsH-4): $Na_3H_{18}B_3W_{39}O_{132}\cdot 56H_2O$ (**NaH-4**) (1 g, 0.094 mmol) was dissolved in water (10 mL). Cesium chloride (0.5 g, 0.1 mmol) was added. The resulting cesium salt was isolated by filtration, washed with ethanol, and dried by rinsing with diethyl ether. Yield: 1.08 g (≈100%). IR (KBr): $\tilde{\nu}$ = 1006(w), 962(m), 855(sh), 829(m), 799(m), 685(m), 383(m), 337 cm^{-1} (m); elemental analysis calcd (%) for $H_{36}Cs_{15}B_3W_{39}O_{147}$: Cs 17.22, B 0.28, W 61.88; found Cs 17.35, B 0.28, W 61.86.

Physical measurements

FT-IR spectroscopy: Infrared spectra were recorded on a Nicolet Magna 550 FT-IR spectrophotometer with samples in pressed KBr pellets. Selected IR spectra of the characteristic compounds **Cs-1**, **$CsNH_4$-3**, and **CsH-4**, along with the IR spectrum of $K_8HBW_{11}O_{39}\cdot 13H_2O$ for comparison, are shown in Figure S1 in the Supporting Information.

^{183}W NMR spectroscopy: ^{183}W NMR spectra (300 K) were recorded from solutions in 10 mm o.d. tubes at 12.5 MHz on a Bruker AC300 spectrometer (**1**, **2**, and **3**) and at 20.8 MHz on a Bruker DRX500 spectrometer equipped with a standard tunable BBO probehead (**4**). Chemical shifts are referenced to 2 mol L^{-1} Na_2WO_4 solution in alkaline D_2O (δ = 0 ppm) according to the IUPAC recommendations: a positive δ corresponds to a high-frequency shift (deshielding) with respect to the reference. They were measured by the substitution method, using a saturated solution of dodecatungstosilicic acid ($H_4SiW_{12}O_{40}$) in D_2O as a secondary standard (δ = −103.8 ppm).

Saturated aqueous solutions of **1**, **2**, and **3** as their sodium salts (**Na-1**, **Na-2**, and **Na-3**, respectively) were obtained by cationic exchange of the corresponding mixed ammonium/cesium salts by means of a Dowex 50W-X2 resin (Na^+-form). The eluate was concentrated to dryness and the residue was redissolved in H_2O/D_2O (1:1) in order to obtain a polyanion concentration of 0.8 mol L^{-1}. The spectra of **Na-1**, **Na-2**, and **Na-3** are shown in Figures S2, S3, and S4 in the Supporting Information, respectively.

For 1D and 2D ^{183}W NMR measurements of **4**, a nearly saturated aqueous solution was prepared by dissolving 6.5 g of the mixed salt **NaH-4** in less than 2 mL of D_2O to give a final volume of about 2.5 mL (ca. 0.25 mol L^{-1}).

The ^{183}W 2D-COSY spectrum was obtained at 20.8 MHz using a simple Jeener (90° – incremental delay – 90° – acquisition – relaxation delay) pulse sequence. The spectral width was 6400 Hz (308 ppm) and 6000 transients were acquired with the sum of acquisition time and relaxation delay amounting to 500 ms. The number of stored experiments (t_1 dimension) was 128, requiring a total spectrometer time of more than three days (75 h). The data were zero-filled and apodized with a sine bell function before Fourier transformation. The resulting COSY map (Figure 6) is presented as a power spectrum after symmetrization of the transformed matrix. Despite the very high concentration of anion **4** in the solution and the significant spectrometer time, the lack of any symmetry of the species and the low receptivity of ^{183}W result in a relatively poor signal-to-noise ratio, which precludes detection of the low-intensity cross-peaks, especially those near the diagonal.

X-ray crystallography: Intensity data collections were carried out at room temperature on a Siemens SMART 1K CCD for **$CsNH_4$-2** and **NaH-4** and on a Bruker X8 APEX2 CCD for **$CsNH_4$-3**, both using the $Mo_{K\alpha}$ wavelength (λ = 0.71073 Å). Crystals of **$CsNH_4$-2**, **$CsNH_4$-3**, and **NaH-4** were mounted in sealed Lindeman tubes to prevent any loss of water of crystallization. An empirical absorption correction was applied using the SADABS program[32] based on the method of Blessing.[33] The structures were solved by direct methods and refined by full-matrix least-squares using the SHELX-TL package.[34] Relevant crystallographic data of compounds **$CsNH_4$-2**, **$CsNH_4$-3**, and **NaH-4** are reported in Table 1; selected bond distances and angles are given in Table 2. The heavier atoms (W and Cs) in each structure were initially located by direct methods. The remaining non-hydrogen atoms were located from Fourier differences and were refined with anisotropic thermal parameters. The disordered atoms, that is, the alkali metal cations and the oxygen atoms of the water of crystallization, were refined isotropically. Further details concerning the crystal structure determinations can be obtained from the Fachinformationszentrum Karlsruhe, 76344 Eggenstein-Leopoldshafen,

Germany (Fax: (+49) 7247–808666; e-mail: crystaldata@fiz-karlsruhe.de) on quoting the depository numbers CSD-417446, CSD-417447, and CSD-417445 for **$CsNH_4$-2**, **$CsNH_4$-3**, and **NaH-4**, respectively.

Acknowledgements

We gratefully acknowledge the Centre National de la Recherche Scientifique (CNRS) and the Ministère de l'Education Nationale de l'Enseignement Supérieur et de la Recherche (MENESR) for their financial support. We thank Dr. Mohamed Ahouas (Institut Lavoisier de Versailles) for recording the NMR spectrum of **3**.

[1] Reviews include the following: *Polyoxometalates: From Platonic Solids to Anti-Retroviral Activity* (Eds.: M. T. Pope, A. Müller), Kluwer Academic Publishers, Dordrecht, The Netherlands, **1994**, pp. 1–141. Special issue of Chemical Reviews on Polyoxometalates (Ed.: C. L. Hill) *Chem. Rev.* **1998**, 98, 1–387. Design of solid polyoxometalate catalysts: M. Misono, *Chem. Commun.* **2001**, 1141–1152.
[2] R. Contant, G. Hervé, *Rev. Inorg. Chem.* **2002**, *22*, 63–111.
[3] M. T. Pope, A. Müller, D. Gatteschi, *Chem. Rev.* **1998**.
[4] M. T. Pope, A. Müller, *Angew. Chem.* **1991**, *103*, 56–70; *Angew. Chem. Int. Ed. Engl.* **1991**, *30*, 34–48.
[5] A. Tézé, G. Hervé, *J. Inorg. Nucl. Chem.* **1977**, *19*, 2152.
[6] H. Copaux, *Ann. Chim.* **1909**, *17*, 217.
[7] M. T. Pope, *Heteropoly and Isopoly Oxometalate*, Springer, Berlin, **1983**, p. 79.
[8] G. Hervé, A. Tézé, *C. R. Acad. Sci. Ser. C* **1974**, *278*, 1417.
[9] F. A. Cotton, G. Wilkinson, *Advanced Inorganic Chemistry*, 4th ed., Wiley, New York, **1980**, p. 296.
[10] H. Fletcher, C. C. Allen, R. C. Burns, D. C. Craig, *Acta Crystallogr. Sect. C* **2001**, 57, 505.
[11] A. Couto, C. Trovao, J. Rocha, A. M. Cavaleiro, J. D. Dejesus, *J. Chem. Soc. Dalton Trans.* **1994**, *17*, 2585.
[12] P. Souchay, *Bull. Soc. Chim. Fr.* **1951**, *5*, 365.
[13] A. Tézé, M. Michelon, G. Hervé, *Inorg. Chem.* **1997**, *36*, 505–509.
[14] G. M. Maksimov, R. I. Maksimovskaya, G. S. Litvak, *Russian J. of Inorg. Chem.* **2005**, *50*, 1062–1065.
[15] A. Tézé, M. Michelon, G. Hervé, *Inorg. Chem.* **1997**, *36*, 5666–5669.
[16] Actually, depending on the experimental conditions (ionic strength, nature of the mixed acid salt or concentration of the polyanion), these lines may be split into single components.
[17] a) C. Brevard, R. Schimpf, G. Tourné, C. M. Tourné, *J. Am. Chem. Soc.* **1983**, *105*, 7059; b) T. L. Jorris, M. Kozik, N. Casañ-Pastor, P. J. Domaille, R. G. Finke, W. K. Miller, L. C. W. Baker, *J. Am. Chem. Soc.* **1987**, *109*, 7402; c) E. Cadot, R. Thouvenot, A. Tézé, G. Hervé, *Inorg. Chem.* **1992**, *31*, 4128.
[18] a) P. J. Domaille, W. H. Knoth, D. C. Roe, *Inorg. Chem.* **1983**, *22*, 818.
[19] G. Lenoble, B. Hasenknopf, R. Thouvenot, *J. Am. Chem. Soc.* **2006**, *128*, 5735.
[20] a) R. Acerete, C. F. Hammer, L. C. W. Baker, *J. Am. Chem. Soc.* **1979**, *101*, 267; b) R. Acerete, C. F. Hammer, L. C. W. Baker, *J. Am. Chem. Soc.* **1982**, *104*, 5384.
[21] L. P. Kazansky, *J. Phys. Chem.* A **2004**, *108*, 6437.
[22] A. Bagno, M. Bonchio, *Chem. Phys. Lett.* **2000**, *317*, 123.
[23] M. H. Alizadeh, S. P. Harmalker, Y. Jeannin, J. Martin-Frère, M. T. Pope, *J. Am. Chem. Soc.* **1985**, *107*, 2662.
[24] R. Acerete, C. F. Hammer, L. C. W. Baker, *Inorg. Chem.* **1984**, *23*, 1478.
[25] R. Acerete, C. F. Hammer, L. C. W. Baker, *J. Am. Chem. Soc.* **1982**, *104*, 5384.
[26] O. A. Duncan, R. K. C. Ho, W. G. Klemperer, *J. Organomet. Chem.* **1980**, *187*, C27.
[27] J. Gracia, J. M. Poblet, J. Autschbach, L. P. Kazansky, *Eur. J. Inorg. Chem.* **2006**, 1139–1148.
[28] The magnitude of $^2J_{W\text{-}O\text{-}W}$ coupling, observed as satellites of the main resonances, depends on the W-O-W angle. $^2J_{W\text{-}O\text{-}W}$ coupling constants are in the range 15–25 Hz for corner junctions (W-O-W $\approx$150°) and about 4–7 Hz for W coupled through edge junctions (W-O-W $\approx$125°).
[29] In the 2D ^{183}W NMR spectrum of **4**, most couplings through edge junctions are too weak to give rise to off-diagonal cross-peaks.
[30] H. Copaux, *Ann. Ch. Phys.*, 8^e série, t. XVII, **1909**.
[31] X. Fang, T. M. Anderson, C. L. Hill, *Angew. Chem. Int. Ed.* **2005**, *44*, 3540–3544.
[32] G. M. Sheldrick, SADABS, Program for scaling and correction of area detector data, University of Göttingen, Germany, **1997**.
[33] R. Blessing, *Acta Crystallogr. Sect. A* **1995**, *51*, 33.
[34] G. M. Sheldrick, *Acta Crystallogr. Sect. A* **1990**, *46*, 467; G. M. Sheldrick, SHELX-TL version 5.03, Software Package for Crystal Structure Determination, Siemens Analytical X-ray Instrument Division, Madison, WI, USA, **1994**.

Received: December 23, 2006
Revised: April 6, 2007
Published online: June 20, 2007

